Ferromagnetism and ferroelectricity in epitaxial BiMnO3 ultra-thin films

G. M. De Luca, D. Preziosi, F. Chiarella, R. Di Capua, S. Gariglio, S. Lettieri, and M. Salluzzo

Advertisement:

Ferromagnetism and ferroelectricity in epitaxial BiMnO$_3$ ultra-thin films

G. M. De Luca,[1,a)] D. Preziosi,[2,3] F. Chiarella,[1] R. Di Capua,[1,2] S. Gariglio,[4] S. Lettieri,[1] and M. Salluzzo[1]

[1]*CNR-SPIN, Complesso Monte S. Angelo, Via Cintia, 80126 Napoli, Italy*
[2]*Dipartimento di Fisica, Università "Federico II" di Napoli, Complesso Monte S. Angelo, Via Cintia, 80126 Napoli, Italy*
[3]*Max Planck Institute of Microstructure Physics, Weinberg 2, 06120 Halle, Germany*
[4]*Département de Physique de la Matière Condensée, Université de Genève, 24 Quai Ernest Ansermet, 1211 Geneva 4, Switzerland*

We studied the ferroelectric and ferromagnetic properties of compressive strained and unstrained BiMnO$_3$ thin films grown by rf-magnetron sputtering. BiMnO$_3$ samples exhibit a two-dimensional cube-on-cube growth mode and a pseudo-cubic structure up to a thickness of 15 nm and of 25 nm when deposited on (001) SrTiO$_3$ and (110) DyScO$_3$, respectively. Above these thicknesses, we observe a switching to a three-dimensional island growth mode and a simultaneous structural change to a (00l) oriented monoclinic unit cell. While ferromagnetism is observed below a T$_C \approx 100$ K for all samples, signatures of room temperature ferroelectricity were found only in the pseudo-cubic ultra-thin films, indicating a correlation between electronic and structural orders. © 2013 AIP Publishing LLC. [http://dx.doi.org/10.1063/1.4818136]

In the last years, the research on multiferroic materials has received a strong impulse because of their potential applications in the area of novel multifunctional devices as well as for the very interesting physics, involving the complex coexistence and coupling of ferroelectric and magnetic orders.[1] BiMnO$_3$ (BMO), which has been widely studied in form of polycrystalline samples, represents an interesting example, since it exhibits ferromagnetism below 100 K, with sizeable magnetic moments of the Mn^{3+} ions comparable to the ones of La$_{0.67}$Sr$_{0.33}$MnO$_3$. In addition, it is believed to be ferroelectric[2] with a monoclinic unit cell crystallizing in the non-centrosymmetric C2 space group ($a = 0.954$ nm, $b = 0.561$ nm, $c = 0.986$ nm, $\beta = 110.7°$).[2] The monoclinic unit cell is composed by the superposition of strongly distorted perovskite units with pseudocubic lattice parameter $a_{pc} = 3.95$ Å. Early first-principles calculations[3] suggested proper ferroelectricity associated to the highly polarized $6s^2$ character of Bi^{3+} (lone pairs), as it happens in BiFeO$_3$. However, the occurrence of ferroelectricity in this system has been challenged by a comparative analysis of electron and neutron diffraction data showing that polycrystalline BMO belongs instead to the centrosymmetric monoclinic C2/c space group, thus incompatible with proper ferroelectricity.[4,5] More recently, Solovyev and Pchelkina[6] proposed improper ferroelectricity of BiMnO$_3$ due to the competition between the ferromagnetic phase and a hidden antiferromagnetic phase, characterized by canted Mn spins and a three-dimensional (3D) orbital order arrangement. The balance between these complex states could be tuned by applying external pressure[7] or epitaxial strain.

In this letter, we report on the growth of high quality BMO films on (001) SrTiO$_3$ (STO), with single TiO$_2$ termination and (110) DyScO$_3$ (DSO) single-crystals. On STO, pseudo-cubic BMO films are characterized by a compressive bi-epitaxial strain (mismatch of -1.1%), while the in-plane matching of BMO on (110) DSO is only slightly compressive (mismatch of -0.15%). The study of strained and unstrained films allowed an analysis of the role of the strain on the ferroelectric and ferromagnetic properties of this material.

The growth of BMO films is very difficult because of the high volatility of bismuth ions. A good control of the deposition parameters is extremely important to avoid the formation of competing phases, like BMO + Mn$_3$O$_4$ and BMO + Bi$_2$O$_{2.5}$, as observed by Lee *et al.*[8] In particular, the temperature and the background oxygen during the physical vapor deposition play an important role on the realization of single phase epitaxial BMO films.

BMO samples were deposited by on-axis rf-magnetron sputtering. The crystal structure and the possible presence of spurious phases were verified by x-ray diffraction (Rigaku D-max and PANalytical X'Pert PRO). Finally, the morphology of the deposited samples was analyzed by contact and non-contact Atomic Force Microscopy (AFM, Park XE100). Differently from other reports,[9–11] we used a stoichiometric target in order to minimize the formation of Bi-rich phases. Optimal growth conditions included a deposition pressure of 150 mTorr, composed by a mixture of Ar and O$_2$, with a 10:1 ratio, a reduced rf power of 30 Watt, and substrate temperatures of 650 °C. We avoided any annealing in high oxygen pressure in order to prevent the stabilization of competing phases. Thus, after the growth, the samples were cooled down to room temperature in the same pressure used during the deposition. The systematic study of the role of deposition parameters on the film properties confirmed that very low oxygen partial pressures during the deposition, very small deposition rates, and not too high deposition temperatures are essential to avoid the formation of secondary phases.

Another parameter playing a major role in the optimization of the BMO thin films was the target-substrate distance:

a)Electronic mail: gabriella.deluca@spin.cnr.it.

in particular, we invariably observed the presence of BiO_x, Mn_2O_3, and (less frequently) Mn_3O_4 phases at target to substrate distances above 30 cm, independently on the thickness of the films.

Figs. 1 and 2 report morphological and structural characterizations, respectively. BMO samples exhibit a critical thickness of 25 nm for films deposited on (110) DSO and of 15 nm for films grown on (001) STO. Below these critical thicknesses, the samples show very flat and ordered terraces separated by 0.4 nm high step-edges (Figs. 1(a) and 1(b)) suggesting layer-by-layer or step-flow growth. Above the critical thickness, we observe a 2D-3D growth mode transition. Thick films are indeed characterized by multi-layered, and well ordered, 3D islands, often associated to screw dislocations, as shown in Figs. 1(c) and 1(d). There is a clear correlation with the structural properties, since we observe a structural transition at the same critical thicknesses: above the critical thickness, the orientation of the films changes from a pseudocubic structure, characterized by the pseudocubic c-axis perpendicular to the substrate (Figs. 2(b) and 2(c)), to a monoclinic structure, where the monoclinic $(001)_m$ family of lattice planes is parallel to the substrate surface (Fig. 2(a)). Below 100 nm, all the samples have high crystalline quality and are characterized by rocking curves, measured on the pseudo-cubic $(002)_{pc}$ and on the monoclinic $(003)_m$ reflections, having full widths at half maximum below 0.05°. Above 100 nm, cracks are created.

Concerning in plane epitaxy, x-ray diffraction maps of the pseudo-cubic (103) plane show that thin BMO films deposited on STO are under compressive strain with the in-plane pseudocubic axes perfectly aligned to the STO lattice and a c-axis of 3.99 Å. The elongated c-axis is in perfect agreement with the expected value, assuming an ideally

strained film and using the classical formula for biaxial strain

$$\frac{\Delta c}{c} = \frac{2\nu}{(1-\nu)}\frac{\Delta a}{a}. \tag{1}$$

Here, ν ($=0.33$) is the BMO Poisson coefficient,[12] and Δa and Δc are the in-plane and out-of-plane lattice variations, respectively. Therefore, we can conclude that pseudo-cubic BMO thin films are characterized by a composition close to the stoichiometric one, since either oxygen or bismuth off-stoichiometry would substantially modify the structural parameters,[13] contrary to our observations. On the other hand, thick films show a monoclinic c-axis which is only slightly shorter than the value expected for relaxed BMO.

Advanced magnetic characterizations have been performed by x-ray Magnetic Circular Dichroism (XMCD), at the ID08 beamline of the ESRF Synchrotron facility. Compared to standard magnetic characterizations, this technique allows a direct and element selective method to measure the magnetic moment of a specific ion in the compound, and it is especially suitable for thin films. First of all, an analysis of the x-ray absorption spectra on the optimized pseudo-cubic BMO films demonstrates that manganese is only in the Mn^{3+} oxidation state. Thus, we can exclude the presence of Mn_3O_4 (Mn^{2+}) spurious phases that could influence the magnetic behavior. The magnetic moment was obtained applying XMCD sum rules,[14] taking into account a correction factor calculated from a reference ferromagnetic $La_{0.75}Sr_{0.25}MnO_3$ sample. This correction factor is necessary, since it is known that the sum rules do not apply exactly to Mn.[15] In Fig. 3, we show the magnetization, measured from 9 K to room temperature, in a magnetic field of 2 T. Both strained and unstrained BMO show a ferromagnetic transition around $T_C = 100$ K, which is similar to the well known bulk value.

The saturation magnetization, M_{sat}, determined from the XMCD data at 8 K and high field (>2 T) is about 2.8 μ_B/Mn and 3.2 μ_B/Mn for films deposited on STO and DSO, respectively. These values are smaller than 4 μ_B/Mn corresponding to fully aligned Mn^{3+}.[4]

To investigate the ferroelectric properties of the films, we have grown BMO on metallic $LaNiO_3$ buffer layers (deposited on STO) by off-axis rf-sputtering at University of Geneva.[16] While the in plane resistivity is very large even at room temperature, in particular for thin pseudo-cubic films, standard ferroelectric test measurements in a sandwich configuration failed due to the high leakage.

For these reasons, evidences of ferroelectric behavior were sought by Piezo-Force Microscopy (PFM) measurements at room temperature. In Fig. 4(a), we show an example of PFM measurement on pseudo-cubic BMO film. Complex geometrical patterns can be effectively written by using the AFM probe and applying different (negative and positive) dc-biases (± 8 V, bright and dark regions in the amplitude of PFM response, see Fig. 4(a)). We did not observe any major difference in the recorded patterns by applying absolute voltages between 3 and 10 V (maximum value allowed by our instrument), which is consistent with the coercive polarization voltage that can be inferred from Fig. 4(b). However, small local differences could be
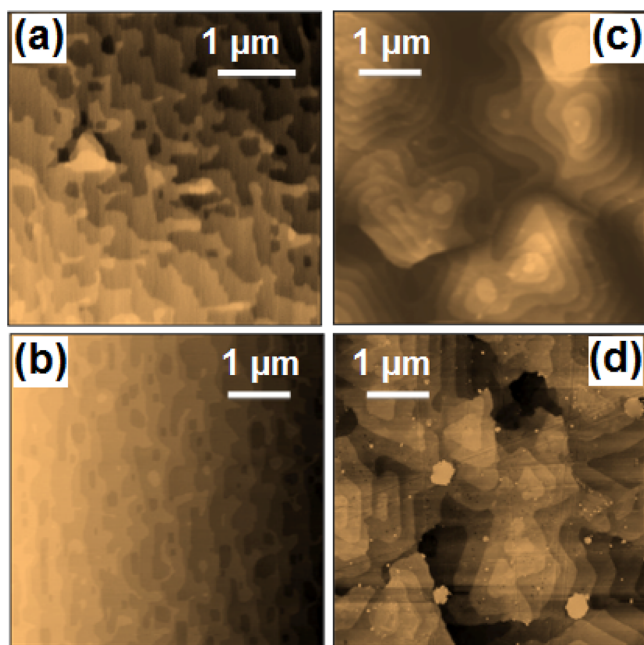

FIG. 1. AFM images of different thickness BMO films grown on STO and DSO substrates: (a) 10 nm-thick BMO on STO (root mean squared (rms) roughness = 0.137 nm); (b) 10 nm-thick BMO on DSO (rms roughness = 0.140 nm); (c) 60 nm-thick BMO on STO (rms roughness = 0.925 nm); (d) 60 nm-thick BMO on DSO (rms roughness = 1.771 nm).
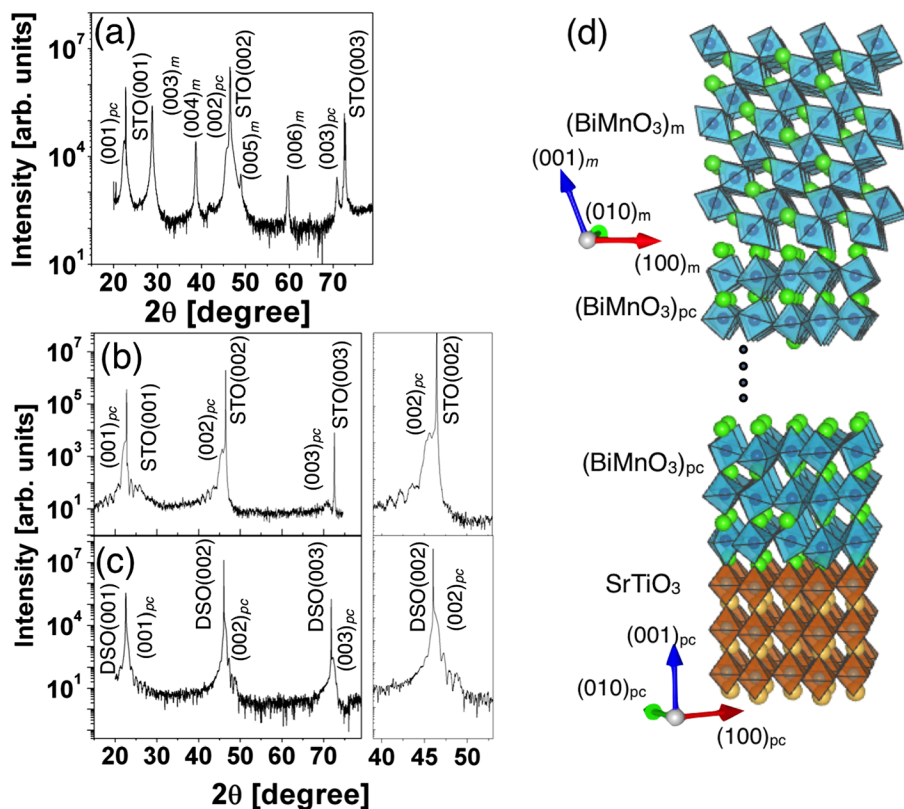
FIG. 2. θ-2θ x-ray diffraction on (a) 60 nm-thick BMO film deposited on (001) STO, (b) 10 nm-thick BMO grown on STO, and (c) 10 nm-thick BMO grown on DSO substrates. Finite size effect oscillations can be observed on the pseudo-cubic films in (b) and (c). (d) A sketch of a plausible structural model of pseudo-cubic and monoclinic BMO deposited on STO.

observed, probably due to local inhomogeneities in the coercive field; the reported image was recorded by applying ± 8 V, which is far from the breakdown voltage and at the same time ensures that all the surface locations were polarized above their local coercive field. We observe all the typical signatures of ferroelectric domain switching, in particular, 180° switching of the phase among regions with reversed polarization and phase/amplitude vs. tip voltage loops typical of ferroelectric materials (Fig. 4(b)).[17] Thus, the PFM response, in both amplitude and phase, can be related to the different signs of a component of the polarization perpendicular to the film surface. However, these results represent a necessary but not a sufficient proof in favor of
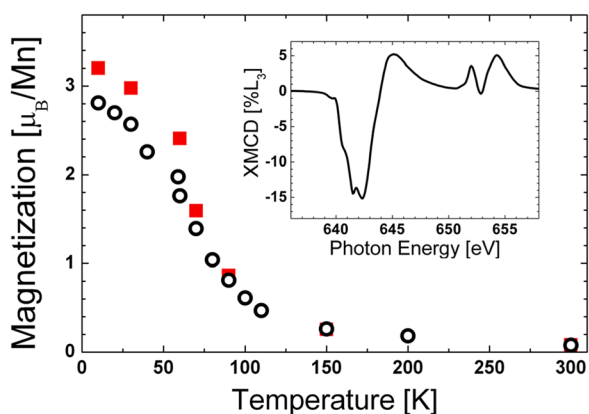

FIG. 3. Temperature dependence of the magnetization obtained using sum rules applied to XMCD spectra acquired on 10 nm-thick BMO films deposited on STO (black open circle) and DSO (full red square). The data have been acquired warming up of the samples from 8 K to 300 K in a field of 2 T, almost parallel to the surface. The inset shows an example of Mn $L_{2,3}$ edge XMCD spectra (10 K, 3 T).
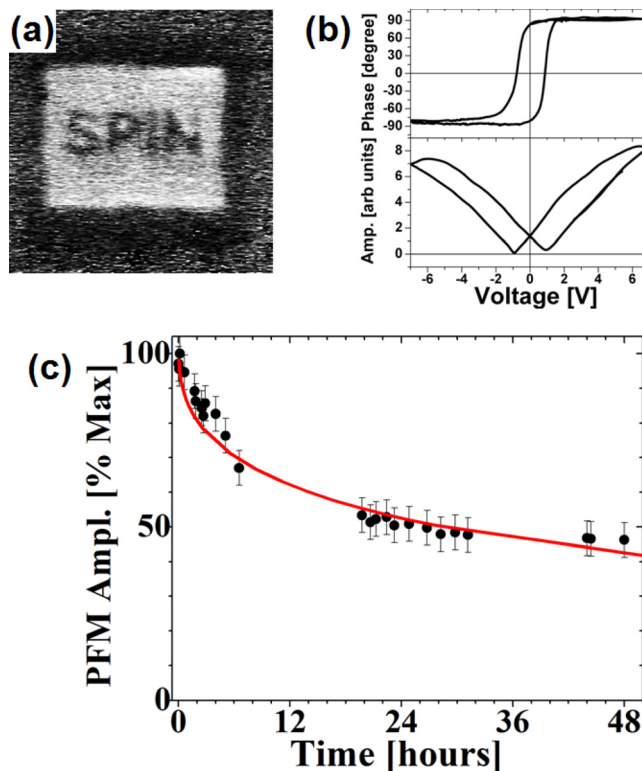

FIG. 4. (a) PFM amplitude image obtained over a $5\,\mu m \times 5\,\mu m$ area on a 10 nm-thick BMO film on STO, showing a complex pattern created by applying positive (bright regions) and negative (dark regions) tip bias voltages of ± 8 V. (b) Phase vs. bias voltage and amplitude vs. bias voltage hysteresis loops obtained on a given location of the sample. (c) PFM amplitude as function of the time acquired on a 10 nm-thick BMO thin film grown on DSO. The red line is a fit using Eq. (2).

room temperature ferroelectricity in our films. As discussed in Ref. 18, there are two possible alternative explanations: (1) simple charging of the surface and (2) ionic displacements of the oxygen ions perpendicular to the surface in a direction defined by the applied electric field.

For this reason, we investigated the time dependence of the amplitude of the piezo-response signal, which is in case of ferroelectric materials proportional to the polarization. In Fig. 4(c), we show the change of the PFM amplitude on a pseudo-cubic 10 nm-thick BMO, after the application of writing tip voltage of ± 8 V. Assuming this signal associated to a loss of polarization of a ferroelectric, our data are well described by a stretched exponential function,[19] as already reported for ferroelectric materials[20]

$$\Delta P(t) = \Delta P_0 \times e^{-\alpha t^\beta}. \tag{2}$$

In Eq. (2), $\Delta P(t)$ and ΔP_0 are the differences at time t and $t = 0$, respectively, between the polarization of polarized and unpolarized surface, α is a constant related to the decay rate, and β is a characteristic exponent equal to 0.42 in our case. We can see that ΔP is about 50% of ΔP_0 after 30 h, and after two days, we still measure a polarization of about 45% of the initial value. We mention that on thick films characterized by a 3D growth mode and a different orientation, we were never able to detect a stable PFM, ferroelectric-like, signal. Thus, these data, even if not conclusive, suggest that pseudo-cubic thin films are indeed ferroelectric at room temperature.

It is worth noting that the main differences between thin and thick BMO concern their structure and their strain state. Thin films are epitaxially strained and have a pseudo-cubic lattice. Unfortunately, we cannot firmly establish, on the base of our lab-based x-ray data, if thin films have a structure belonging to centrosymmetric or non-centrosymmetric space groups. However, the structural distortions induced by the substrate are very likely sufficient to make these samples substantially different from relaxed monoclinic BMO. On the other hand, thick films are relaxed and consequently have structural properties closer to bulk BMO. Thus, we attribute the ferroelectric behavior observed in strained pseudo-cubic BMO films to their structure. Clear signatures of ferroelectric behavior at room temperature were previously observed only in BMO heterostructures employing STO separation layers between BMO films and metallic electrodes.[21] On the other hand, systematic studies of BMO and La-doped BMO provided evidence that ferroelectricity is stabilized by La-substitution of volatile Bi ions,[22] which also influence the unit cell structure.[23] Our data suggest that the epitaxial distortion of the monoclinic BMO unit cell is the driving force for the observed behavior. More investigations, using advanced spectroscopy, are then required to establish whether crystalline pseudocubic BMO films are also multiferroic.

In conclusion, we found the right deposition condition to grow high quality single phase and extremely flat, ferromagnetic BMO thin films, with single crystal orientation using rf-magnetron sputtering. Piezo-force microscopy reveals that pseudo-cubic thin films are characterized by a ferroelectric-like switching and that the structural order plays an important role in the ferroelectric behavior of these films. These results are promising in view of future investigation of multiferroic effects in strongly ferromagnetic $BiMnO_3$.

[1]S. Picozzi and C. Ederer, J. Phys.: Condens. Matter **21**, 303201 (2009).
[2]A. M. dos Santos, A. K. Cheetham, T. Atou, Y. Syono, Y. Yamaguchi, K. Ohoyama, H. Chiba, and C. N. R. Rao, Phys. Rev. B **66**, 064425 (2002).
[3]N. Hill and K. Rabe, Phys. Rev. B **59**, 8759 (1999).
[4]A. A. Belik, S. Iikubo, T. Yokosawa, K. Kodama, N. Igawa, S. Shamoto, M. Azuma, M. Takano, K. Kimoto, Y. Matsui, and E. Takayama-Muromachi, J. Am. Chem. Soc. **129**, 971 (2007).
[5]E. Montanari, G. Calestani, L. Righi, E. Gilioli, F. Bolzoni, K. S. Knight, and P. G. Radaelli, Phys. Rev. B **75**, 220101 (2007).
[6]I. Solovyev and Z. Pchelkina, Phys. Rev. B **82**, 094425 (2010).
[7]D. P. Kozlenko, A. A. Belik, S. E. Kichanov, I. Mirebeau, D. V. Sheptyakov, T. Strassle, O. L. Makarova, A. Belushkin, B. N. Savenko, and E. Takayama-Muromachi, Phys. Rev. B **82**, 014401 (2010).
[8]J. H. Lee, X. Ke, R. Misra, J. F. Ihlefeld, X. S. Xu, Z. G. Mei, T. Heeg, M. Roeckerath, J. Schubert, Z. K. Liu, J. L. Musfeldt, P. Schiffer, and D. G. Schlom, Appl. Phys. Lett. **96**, 262905 (2010).
[9]E. E. Kaul, N. Haberkorn, and J. Guimpel, Appl. Surf. Sci. **254**, 160 (2007).
[10]E. Langenberg, M. Varela, M. V. Garcia-Cuenca, C. Ferrater, F. Sanchez, and J. Fontcuberta, Mater. Sci. Eng., B **144**, 138 (2007).
[11]W. Eerenstein, F. D. Morrison, J. F. Scott, and N. D. Mathur, Appl. Phys. Lett. **87**, 101906 (2005).
[12]Z.-G. Mei, S. L. Shang, Y. Wang, and Z. K. Liu, J. Phys.: Condens. Matter **22**, 295404 (2010).
[13]A. Sundaresan, R. V. K. Mangalam, A. Iyo, Y. Tanaka, and C. N. R. Rao, J. Mater. Chem. **18**, 2191 (2008).
[14]C. T. Chen, Y. U. Idzerda, H.-J. Lin, N. V. Smith, G. Meigs, E. Chaban, G. H. Ho, E. Pellegrin, and F. Sette, Phys. Rev. Lett. **75**, 152 (1995).
[15]C. Piamonteze, P. Miedema, and F. M. F. de Groot, Phys. Rev. B **80**, 184410 (2009).
[16]R. Scherwitzl, S. Gariglio, M. Gabay, P. Zubko, M. Gibert, and J. M. Triscone, Phys. Rev. Lett. **106**, 246403 (2011).
[17]S. V. Kalinin, A. N. Morozovska, L. Q. Chen, and B. J. Rodriguez, Rep. Prog. Phys. **73**, 056502 (2010).
[18]C. W. Bark, P. Sharma, Y. Wang, S. H. Baek, S. Lee, S. Ryu, C. M. Folkman, T. R. Paudel, A. Kumar, S. V. Kalinin, A. Sokolov, E. Y. Tsymbal, M. S. Rzchowski, A. Gruverman, and C. B. Eom, Nano Lett. **12**, 1765 (2012).
[19]D. C. Johnston, Phys. Rev. B **74**, 184430 (2006).
[20]J. W. Hong, W. Jo, D. C. Kim, S. M. Cho, H. J. Nam, H. M. Lee, and J. U. Bu, Appl. Phys. Lett. **75**, 3183 (1999).
[21]J. Y. Son and Y. H. Shin, Appl. Phys. Lett. **93**, 062902 (2008).
[22]M. Gajek, M. Bibes, S. Fusil, K. Bouzehouane, J. Fontcuberta, A. Barthelemy, and A. Fert, Nature Mater. **6**, 296 (2007).
[23]M. Gajek, M. Bibes, F. Wyczisk, M. Varela, J. Fontcuberta, and A. Barthelemy, Phys. Rev. B **75**, 174417 (2007).